AIP | Journal of Applied Physics

Reverse boundary layer capacitor model in glass/ceramic composites for energy storage applications

Xiaoyong Wei, Haixue Yan, Tong Wang, Qingyuan Hu, G. Viola et al.

Citation: J. Appl. Phys. **113**, 024103 (2013); doi: 10.1063/1.4775493
View online: http://dx.doi.org/10.1063/1.4775493
View Table of Contents: http://jap.aip.org/resource/1/JAPIAU/v113/i2
Published by the AIP Publishing LLC.

Reverse boundary layer capacitor model in glass/ceramic composites for energy storage applications

Xiaoyong Wei,[1,2,a)] Haixue Yan,[1] Tong Wang,[2] Qingyuan Hu,[2] G. Viola,[1,3] Salvatore Grasso,[1,3] Qinghui Jiang,[1] Li Jin,[2] Zhuo Xu,[2] and Michael J. Reece[1,3]
[1]*School of Engineering and Material Science, Queen Mary University of London, London E1 4NS, United Kingdom*
[2]*Electronic Materials Research Laboratory, Key Laboratory of the Ministry of Education & International Center for Dielectric Research, Xian Jiaotong University, Xian 710049, China*
[3]*Nanoforce Technology Ltd, Mile End Road, London E1 4NS, United Kingdom*

(Received 27 October 2012; accepted 18 December 2012; published online 10 January 2013)

Reverse boundary layer capacitor (RBLC) configuration model, where the grain boundary has a higher electrical conductivity than the grain, is proposed in glass/ceramic composites for dielectric energy storage applications. By introducing glass additives as grain boundaries with electrical conductivity higher than ceramic grains, the steady electric field across grains can be larger than grain boundaries as desired due to the conductivity difference. The breakdown field is thus expected to increase in the RBLC-type brick wall model because of the field distribution. The equivalent circuit, grain boundary conductivity dependence of energy density, low-loss frequency range of the RBLC model are discussed. The simulation results suggest that the RBLC approach has advantages in overall energy density, compared with normal insulating glass phase composites.
 [http://dx.doi.org/10.1063/1.4775493]

INTRODUCTION

High density energy storage materials and the related devices have attracted increasing scientific, industrial, and public attention since the energy crisis became more serious in the new century. Renewable energy resources, such as solar and wind energy, are preferably transformed into electric energy for the purpose of storage. There are growing needs for mobile and energy storage devices that are small size, light weight, low cost, and environmentally friendly, for application in transportation, electronics, and aerospace engineering. Dielectric energy storage is the most attractive and feasible way to store and release energy compared to other techniques like mechanical or chemical storage. Capacitors, used in high power applications, have the advantages of high power density (~GW/kg for ceramic capacitor) and long cycling lifetime ($>10^6$ cycles), but the disadvantage of low energy density (1 J/cm^3 for polypropylene thin film capacitors) compared with chemical batteries (>600 J/cm^3 for commercial lithium battery).

Significant research activity has been focused on developing new capacitive materials with higher energy density. The density is proportional to the permittivity ε_r and the square power of the applied electric field E^2 ($E < E_B$, E_B is the breakdown field) for linear dielectrics. Unfortunately, higher permittivity materials always exhibit lower breakdown field.[1] Lower permittivity dielectrics, such as $CaTiO_3$-$CaHfO_3$, possess higher energy density (9.5 J/cm^3) because of the dominance of $E_B{}^2$.[2] For nonlinear dielectrics, e.g., ferroelectric ceramics like $BaTiO_3$, the energy density mainly depends on the maximum polarization, the maximum field, and the remnant polarization. The E_B of bulk ferroelectric ceramics is significantly lower than that of films, normally leading to lower energy density, with typical values as 1.14 J/cm^3 for $Ba_{0.4}Sr_{0.6}TiO_3$/MgO composites,[3] 3.9 J/cm^3 for ZnO doped $Ba_{0.3}Sr_{0.7}TiO_3$ (Ref. 4), and 0.51 J/cm^3 for bismuth based anti-ferroelectric ceramics.[5] In thin films, the breakdown field increases because of the lower defect density. An energy density of 14.5 J/cm^3 was achieved in Sr doped $PbZrO_3$ thin film capacitor,[6] and 37 J/cm^3 in La doped lead zirconate titanate (PLZT) thin film capacitor grown on nickel foils with lanthanum nickel oxide buffer by chemical solution deposition.[7] Nevertheless, these energy density values for inorganic thin films have less practical meaning since the overall energy density (OED) is much lower when one also considers the volume of the substrate. The mass production of thin films is relatively difficult. Multilayer capacitor, in which the dielectric layer thickness is not so large, seems to be a promising candidate for practical energy storage. Relatively high density values (~6.1 J/cm^3) were reported in $BiScO_3$-$BaTiO_3$ thick film capacitors (9 μm dielectric layer thickness).[8]

Compared with inorganic thin films, freestanding polymer films can be produced in large quantities and are currently used in commercial high voltage high power capacitors. The energy density of polymer ferroelectric polyvinylidene fluoride (PVDF) thin films is much higher than that of ferroelectric ceramics due to the high breakdown field, e.g., Zhang's group in Penn State has made remarkable progress in PVDF copolymer (>16 J/cm^3, breakdown field around 500 MV/m).[9] It seems attractive to prepare composites consisting of a polymer matrix with high electric breakdown field and high permittivity ceramic phase to further increase the energy density. However, the results are not as good as expected,[10–13] with some exceptions where anisotropic fillers are used.[14,15]

[a)]Author to whom correspondence should be addressed. Electronic mail: wdy@mail.xjtu.edu.cn.

Generally, the addition of inorganic ceramic phase increases the permittivity, while the breakdown field decreases remarkably, due to the existence of interfacial defects. The defects present at the ceramic-polymer interface are caused by the imperfect wetting and adhesion between organic and inorganic compounds. Additionally, the electric displacement D continuity across the polymer-ceramics interface is satisfied, so that the average field in the polymer is much larger than that of ceramic particles due to the lower permittivity and conductivity. For these two reasons, the nominal breakdown field decreases compared to pure matrix phase, and consequently, the energy density decreases. Furthermore, the interfacial polarization, caused by the difference in the electrical conductivity and permittivity of grain and grain boundary, increases energy loss.[16]

Electrical breakdown is a failure phenomenon analogous with mechanical breakdown. In the mechanical case, the fracture starts from micro cracks, in which the local stress concentration dominates. In electrical case, field concentration can be found in the vicinity of pores, electrode edge, and other structural defects. Therefore, to increase the breakdown field, it is necessary either to eliminate defects or to reduce the field concentration near defects. In order to reduce defects concentration glass-ceramic composites are preferred, since the glass-ceramic composites are more advantageous than ceramic-polymer composites in eliminating interfacial defects because of the absence of organic-inorganic interfaces. It is relatively easy to achieve pore free, highly densified glass-ceramic composites via melting-recrystallization methods,[17–19] or alternatively by glass aided sintering.[20,21] Ordinary silica based glasses possess higher resistivity and lower dielectric permittivity than ferroelectric ceramics,[22] therefore, the energy density of glass ceramic composite, even highly densified, is lower than pure glass,[23] because of the uneven field distribution.

A reverse boundary layer capacitor (RBLC) model is proposed to achieve optimum field distribution, leading to high breakdown field and high energy density in glass ceramics, by introducing glass phase as grain boundaries with an electrical conductivity one or two order of magnitude higher than the ceramic grains. The existence of a low loss frequency region opens up the possibility of applications in high power energy storage. This principle is not only limited to ordinary ferroelectric glass ceramics but also applicable to relaxor ferroelectrics, antiferroelectrics, and polymer based composites.

MODEL

In the well known boundary layer capacitor (BLC), the Maxwell-Wagner interfacial polarization near the insulating grain boundaries leads to large permittivity but lower breakdown field, which is not suitable for energy storage. Therefore, we propose a reverse configuration, reverse boundary layer capacitor, defined by the fact that grain boundaries are more conductive than the grains. The low resistivity glass phase is used as the grain boundary component, which ensures that the voltage drop is mainly applied to the high permittivity grains, and the optimum field distribution is obtained. Furthermore, the existence of an appropriate electrical conductive glass phase would be helpful in releasing the field concentration, either around defects or near surface and cusp. Similar techniques are widely adopted in the high voltage insulation industry.

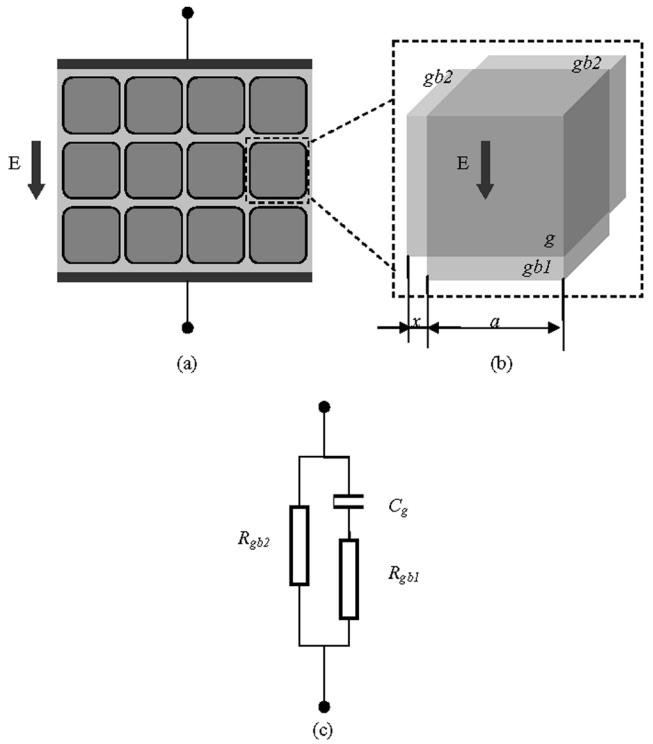

FIG. 1. Schematics of RBLC brick wall model (a) and its basic unit (b) for glass ceramics, where g stands for ferroelectric grain, and gb1/gb2 stand for the glass grain boundaries in serial/parallel with the grain. The geometry of grain and grain boundary are a and x, respectively. E is the electric field. The reduced equivalent circuit (c) of a basic unit is also presented in case of high conductivity glass.

For simplicity purpose, a brick wall model, with ordered cubic grains and consequently regular grain boundaries, is shown in Fig. 1(a). In this context, the effective dielectric constant of a glass ceramic can be analyzed using a complex 3-D parallel and serial network of a basic unit, which is

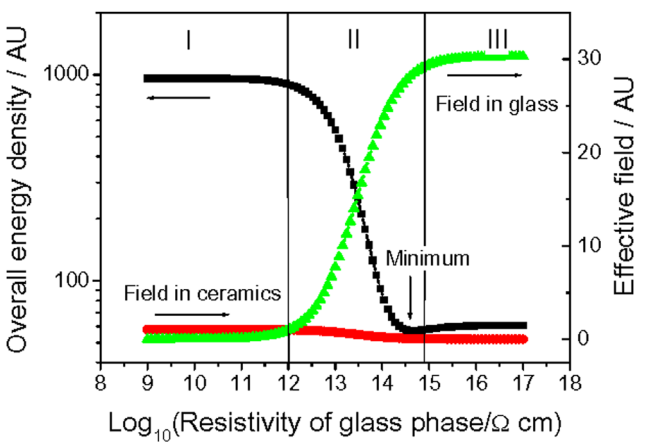

FIG. 2. Calculated overall energy density and effective fields in ceramic grains and glass grain boundaries in series with grains, as functions of glass resistivity. The typical parameters used are: x/a = 1/30; $\varepsilon_g = 1000$; $\varepsilon_{gb} < 10$; $\rho_g = 10^{12}$ Ω cm; $\rho_{gb} = 10^9$-10^{17} Ω cm, for 10% glass volume fraction.

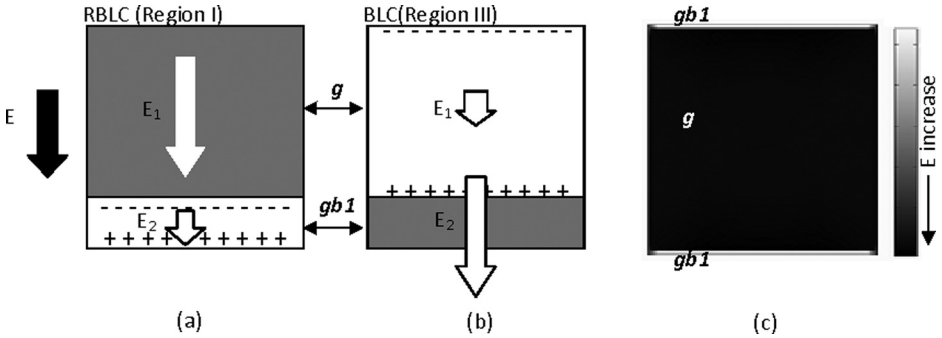

FIG. 3. The schematic drawings of electric field in grain and grain boundary (gb1) for RBLC (a) and BLC (b) models. The longer arrow indicates larger field. The "−" and "+" indicate negative and positive accumulated interfacial space charges, respectively. The simulated electric field plot for RBLC (c) is shown for comparison, where the parameters are the same with those in Figure 2 and ρ_{gb} is fixed to $10^9\ \Omega$ cm.

considered as a combination of one cubic grain and three pieces of thin plate grain boundaries (in sense of periodicity). The dimensions of the cube and the plate are a and x, respectively, as shown in Fig. 1(b). In case of small volume fraction of glass phase, x is much smaller than a (e.g., $x/a \approx 1/30$ for 10% volume fraction of glass phase). The contributions from the fringe and corner parts are omitted.

The equivalent circuit of the above basic unit is complex if one tries to calculate the exact field distribution rigorously in the brick wall composite. Approximately, it can be reduced to a combination of several parallel R-C components, i.e., R_g-C_g for grains in series with R_{gb1}-C_{gb1} for grain boundary 1 and further in parallel with R_{gb2}-C_{gb2} for grain boundary 2. Provided the grain boundary has higher conductivity, the equivalent circuit can be further reduced to a lossy Debye type, where C_g, R_{gb1}, and R_{gb2} are predominant as shown in Fig. 1(c). Notice the conductivity contrast here is contrary to the so called BLC, where grain boundary is more insulating than grain, leading to interfacial Maxwell-Wagner polarization and giant permittivity.

DISCUSSION

The field distribution and overall energy density of a typical glass ceramic are calculated based on the above brick wall model. At steady state, the current flow across the grain-boundary interface is constant, i.e., the electric fields E_i in each phase can be determined using this continuity. The fields in grain and grain boundary can be calculated by a simple serial model of resistor layers, $E_i = \rho_i E(\sum d_j)/(\sum \rho_j d_j)$ (i, j = 1, 2), in which E is the nominal field, ρ_j and d_j are electrical resistivity and thickness of the jth components, respectively, are shown in Fig. 2 as a function of the resistivity of the glassy grain boundary for a model system (see figure caption for the materials properties used). The overall energy density is calculated by $OED = \sum \frac{1}{2} y_i \varepsilon_i E_i^2$, where y_i, ε_i, and E_i are the volume fraction, permittivity, and electric field of the ith component, with the latter depending on the electrical resistivity of grains and grain boundaries, as shown above. Figure 2 shows the OED as a function of the resistivity of the glassy grain boundary ($\rho_{gb} = 10^9$-$10^{17}\ \Omega$ cm), by fixing the permittivity of grain ($\varepsilon_g = 1000$) and grain boundary ($\varepsilon_{gb} < 10$) and the volume fraction of glassy phase (10 vol. %). Here, the parallel grain boundary (gb2) is simply ignored because its contribution to energy density is always negligible compared with that of grain.

Figure 2 exhibits three distinctive regions. Region I corresponds to a high conductivity glass and hence the RBLC region, where the energy density is the highest and the average field in both the ferroelectric phase and the glass phase are low. Region III corresponds to a low conductivity glass and BLC region, where the energy density is the lowest (1/16 of the highest value in region I) and the average field in glass phase is much higher (30 times higher than the field in region I). Region II is a transitional dispersion region in between, where the energy density and average field in both ceramic and glass phases change significantly with glass conductivity, and interestingly the energy density exhibits a minimum at a relatively higher resistivity ($\sim 10^{14}$ to $10^{15}\ \Omega$ cm). Arbitrary units are used in the figure just for comparison. Schematic drawings of the field comparison for region I and II are shown in Figs. 3(a) and 3(b). Finite element analysis results of the region I (RBLC) are shown in Fig. 3(c), which is in accordance with Fig. 3(a), e.g., field in grain is stronger than that in grain boundary.

The ideal energy density for ferroelectric ceramics should be high provided its E_B can be increased to an intrinsic value (the ideal defect free condition), as those found in thin films for very small thickness ($<1\ \mu$m). The high conductivity grain boundaries (gb1) help to archive homogeneous electric field in high voltage applications. Consequently, in case of fine grain glass-ceramics, the E_B value of RBLC type glass ceramics is expected to increase towards the intrinsic value of the grain/ceramic phase. The corresponding

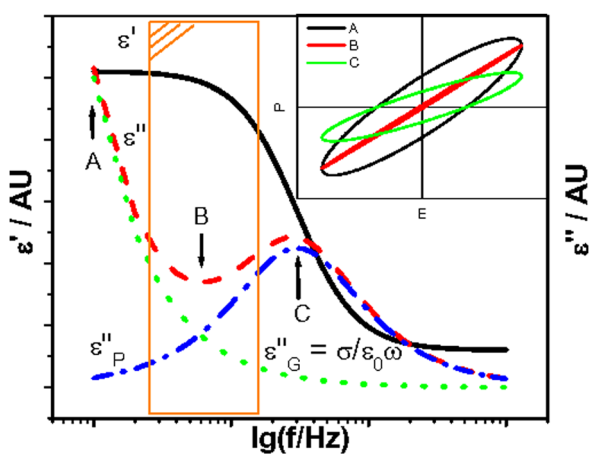

FIG. 4. Frequency dependence of the effective permittivity for the RBLC model. The shaded area is a low loss region where both the polarization loss ε''_P and conductive loss ε''_G are relatively low. The inset shows simulated P-E loops at different frequency point A, B, and C shown in the figure. Material and structure properties used are same with Figure 2, except for grain boundary resistivity $\rho_{gb} = 10^9\ \Omega$ cm.

TABLE. I. Calculated values for RBLC model ($\varepsilon_g = 1000$; $\varepsilon_{gb} < 10$; $\rho_g = 10^{12}\ \Omega$ cm).

Volume fraction of glass phase (%)	x/a	Resistivity of glass phase (Ω cm)	$tg\delta_{min}$	$tg\delta_{min}$ frequency (Hz, angular)	Relaxation frequency[a] (Hz, angular)	Self-discharge time[b] (s)
3	0.010	10^9	<0.03	15	10^3	5
		10^{11}		0.15	10	500
10	0.033	10^9	<0.1	15	300	1.5
		10^{11}		0.15	3	150

[a]Relaxation frequency is calculated from the reciprocal of serial RC product $(C_gR_{gb1})^{-1}$, $\omega_r = a/(x\varepsilon_0\varepsilon_g\rho_{gb})$.
[b]Self-discharge time is calculated by the parallel RC product $C_gR_{gb2} = a^2/(2\omega_r x^2)$.

glass ceramic structure seems to be feasible approach for mass production of high energy storage material.

With the addition of low resistivity component (region I in Fig. 2), the dielectric loss is inevitably increased. Based on the equivalent circuit analysis, the frequency dependence can be simulated as shown in Fig. 4. It is similar to a lossy Debye system, where the ε'' contains two parts, ε_P'' relative to the grain boundary in series with the grain (gb1) (subs. P stands for polarization loss induced by R-C relaxation) and ε_G'' relative to the grain boundary in parallel with the grain (gb2), (subs. G stands for conduction loss), according to the configuration shown in Fig. 1. The intrinsic dielectric loss of the grain is ignored here for simplicity. These values are calculated from the equivalent circuit, showing different frequency dependences, therefore, it is possible to have a low loss area in the medium frequency range, as highlighted by the shaded area shown in Fig. 4, where slim P-E loop can be expected (curve B shown in inset). The frequency range is adjustable by changing the material parameters, especially the resistivity of the grain boundary phase. Furthermore, as indicated in Fig. 2, this RBLC mechanism is still valid for very insulating glass phase, only if the resistivity of the glass phase is one order of magnitude lower than that of the grain, when x/a ratio is about 1/30. This is an important implication for obtaining low loss materials for certain high power application, such as secondary power source (power cache) in electric vehicles.

Table I shows some typical material parameters and the corresponding calculated energy storage properties. The minimum loss tangent is 0.03 for x/a = 0.01, and the corresponding frequency (15 Hz, angular) is far from either the relaxation frequency (1kHz, angular, calculated by $\omega_r = (C_gR_{gb1})^{-1} = a/(x\varepsilon_0\varepsilon_g\rho_{gb})$) or reciprocal of self-discharging time (5 s, corresponding to 0.2 Hz, angular, calculated by $\tau = C_gR_{gb2} = a^2/(2\omega_r x^2)$, see Table I), serving as the upper and lower frequency limits. Although there is no direct grain size term in the OED calculation equation, the overall energy density would still have strong grain size dependence, because the material properties, such as E_B and ε, are size sensitive. Furthermore, the low loss frequency range is also size dependent, which is obvious from the relaxation frequency and self-discharging time expressions. Therefore, scaling down may be useful for the RBLC and for the energy density enhancement. Of course, other effects induced by the scaling down should be considered, e.g., polarization decrease and switching field increase.

The high permittivity phase can be ferroelectric, relaxor ferroelectric, or antiferroelectric. Ferroelectrics have large remnant polarization (P_r), which hinders energy release. Relaxor ferroelectrics have lower P_r, so the energy triangle could be larger. Antiferroelectrics have different polarization behavior, the P_r is close to zero, and the phase transformation field is high (e.g., 50 MV/m), leading to high energy storage density (14.5 J/cm^3).[6] Again, because of the uneven field distribution, the antiferroelectric to ferroelectric phase transformation cannot occur in insulating polymer composites, however, it is possible to have the phase transformation in RBLC glass ceramics according to the discussions above. This opens up the possibility of taking advantage of using antiferroelectrics, as well as relaxor ferroelectrics for high energy storage systems.

CONCLUSIONS

A reverse boundary layer capacitor model is proposed to achieve optimum field distribution, leading to high breakdown field and high energy density in glass ceramics, by introducing glass phase as grain boundaries with an electrical conductivity one or two order of magnitude higher than the ceramic grains. The existence of a low loss frequency region opens up the possibility of applications in high power energy storage. This principle is not only limited to ordinary ferroelectric glass ceramics but also applicable to relaxor ferroelectrics, antiferroelectrics, and polymer based composites.

ACKNOWLEDGMENTS

This work was supported by the Marie Curie Fellowship from FP7 framework of European Union (XYW).

[1]G. Ribes, J. Mitard, M. Denais, S. Bruyere, F. Monsieur, C. Parthasarathy, E. Vincent, and G. Ghibaudo, IEEE Trans. Device Mater. Reliab. **5**, 5 (2005).
[2]D. P. Shay, N. J. Podraza, N. J. Donnelly, and C. A. Randall, J. Am. Ceram. Soc. **95**, 1348 (2012).
[3]Q. Zhang, L. Wang, J. Luo, Q. Tang, and J. Du, Int. J. Appl. Ceram. Technol. **7**, E124 (2010).
[4]G. Dong, S. Ma, J. Du, and J. Cui, Ceram. Int. **35**, 2069 (2009).
[5]G. Viola, H. Ning, M. J. Reece, R. Wilson, T. M. Correia, P. Weaver, M. G. Cain, and H. Yan, J. Phys. D: Appl. Phys. **45**, 355302 (2012).
[6]X. H. Hao, J. W. Zhai, and X. Yao, J. Am. Ceram. Soc. **92**, 1133 (2009).
[7]B. H. Ma, D.-K. Kwon, M. Narayanan, and U. B. Balachandran, J. Mater. Res. **24**, 2993 (2009).
[8]H. Ogihara, C. A. Randall, and S. Trolier-McKinstry, J. Am. Ceram. Soc. **92**, 1719 (2009).
[9]B. J. Chu, X. Zhou, K. L. Ren, B. Neese, M. R. Lin, Q. Wang, F. Bauer, and Q. M. Zhang, Science **313**, 334 (2006).

[10]M. Arbatti, X. Shan, and Z. Cheng, Adv. Mater. **19**, 1369 (2007).
[11]Z. Dang, Y. Shen, and C. W. Nan, Appl. Phys. Lett. **81**, 4814 (2002).
[12]J. Y. Li, L. Zhang, and S. Ducharme, Appl. Phys. Lett. **90**, 132901 (2007).
[13]J. Li, P. Khanchaitit, K. Han, and Q. Wang, Chem. Mater. **22**, 5350 (2010).
[14]V. Tomer and C. A. Randall, J. Appl. Phys. **104**, 074106 (2008).
[15]S. P. Fillery, H. Koerner, L. Drummy, E. Dunkerley, M. F. Durstock, D. F. Schmidt, and R. A. Vaia, ACS Appl. Mater. Interfaces **4**, 1388 (2012).
[16]M. J. Pan, E. P. Gorzkowski, B. A. Bender, and C. C. M. Wu, in *Proceedings of the. 15th IEEE International Symposium on Applications of Ferroelectrics* (2006), p. 25.
[17]J. Luo, J. Du, Q. Tang, and C. Mao, IEEE Trans. Electron Devices **55**, 3549 (2008).
[18]E. P. Gorzkowski, M.-J. Pan, B. Bender, and C. C. M. Wu, J. Electroceram. **18**, 269 (2007).
[19]M. J. Reece, C. A. Worrell, G. J. Hill, and R. Morrell, J. Am. Ceram. Soc. **79**, 17 (1996).
[20]X. Wang, Y. Zhang, X. Song, Z. Yuan, T. Ma, Q. Zhang, C. Deng, and T. Liang, J. Eur. Ceram. Soc. **32**, 559 (2012).
[21]K. Chen, Y. Pu, N. Xu, and X. Luo, J. Mater. Sci.: Mater. Electron. **23**, 1599 (2012).
[22]W. D. Callister, Jr. and D. G. Rethwisch, *Materials Science and Engineering: An Introduction*, 8th ed. (Wiley, New York, 2009).
[23]N. J. Smith, B. Rangarajan, M. T. Lanagan, and C. G. Pantano, Mater. Lett. **63**, 1245 (2009).